Published in final edited form as:
Phys Med Biol. 2011 February 7; 56(3): 703–719.

Radiobiological characterization of post-lumpectomy focal brachytherapy with lipid nanoparticle-carried radionuclides

Brian A Hrycushko[1], **Alonso N Gutierrez**[2], **Beth Goins**[1], **Weiqiang Yan**[1], **William T Phillips**[1], **Pamela M Otto**[1], and **Ande Bao**[1,3]

[1] Department of Radiology, University of Texas Health Science Center at San Antonio, San Antonio, TX, USA

[2] Department of Radiation Oncology, University of Texas Health Science Center at San Antonio, San Antonio, TX, USA

[3] Department of Otolaryngology—Head and Neck Surgery, University of Texas Health Science Center at San Antonio, San Antonio, TX, USA

Abstract

Post-operative radiotherapy has commonly been used for early stage breast cancer to treat residual disease. The primary objective of this work was to characterize, through dosimetric and radiobiological modeling, a novel focal brachytherapy technique which uses direct intracavitary infusion of β-emitting radionuclides (^{186}Re/^{188}Re) carried by lipid nanoparticles (liposomes). Absorbed dose calculations were performed for a spherical lumpectomy cavity with a uniformly injected activity distribution using a dose point kernel convolution technique. Radiobiological indices were used to relate predicted therapy outcome and normal tissue complication of this technique with equivalent external beam radiotherapy treatment regimens. Modeled stromal damage was used as a measure of the inhibition of the stimulatory effect on tumor growth driven by the wound healing response. A sample treatment plan delivering 50 Gy at a therapeutic range of 2.0 mm for ^{186}Re-liposomes and 5.0 mm for ^{188}Re-liposomes takes advantage of the dose delivery characteristics of the β-emissions, providing significant EUD (58.2 Gy and 72.5 Gy for ^{186}Re and ^{188}Re, respectively) with a minimal NTCP (0.046%) of the healthy ipsilateral breast. Modeling of kidney BED and ipsilateral breast NTCP showed that large injected activity concentrations of both radionuclides could be safely administered without significant complications.

1. Introduction

More early stage breast cancers with small primary lesions have been diagnosed through increased use of screening and diagnostic mammography; thus, breast-conserving surgery has replaced the mastectomy gold standard. An improved cosmetic outcome and overall quality of life stemming from the less extensive surgery is a significant benefit at the expense of a potential increased risk in local recurrence (Fisher *et al* 2002). However, the addition of adjuvant radiotherapy has proven in many trials to give similar local recurrence rates for the combined modalities as that of mastectomy alone, ranging from 2.3% to 10% for mastectomy and 2.7% to 8.5% for breast conserving surgery followed by radiotherapy over 10 to 20 years (Blichert-Toft *et al* 2008, Fisher *et al* 2002, Liljegren *et al* 1999,

Correspondence to: Ande Bao.
bao@uthscsa.edu .

Veronesi *et al* 2002). This suggests residual disease following breast-conserving surgery contributes to recurrences. Although similar recurrence rates, it has been described that over 90% of recurrences following lumpectomy and adjuvant radiotherapy are within or in close proximity to the tumor bed and surgical scar (Tobias *et al* 2006). Possible explanations for the close location include: (1) tumour cell shedding during excision, which is indicated from cavity lavage cytology and re-excisions (Motomura *et al* 1999, Sabel *et al* 2009); (2) incomplete removal or missed tumor, possibly due to breast duct anatomy and an extensive intraductal component (Mannino and Yarnold 2009, Holland *et al* 1990); (3) stimulation of migration and growth of residual occult tumor cells through the wound healing response (Hockel and Dornhofer 2005, Belletti *et al* 2008, Tagliabue *et al* 2003).

These findings suggest dose escalation to the tumor bed region may decrease the probability of a proximal recurrence. High focal irradiation may be used to sterilize residual tumour and inhibit activation of intracellular transduction pathways that initiate wound-healing mechanisms characterized by angiogenesis, fibroplasia, collagen production and granulation tissue formation. In fact, tumor bed dose escalation trials have been proven to reduce local recurrence rates, and new methods of partial breast irradiation and tumor bed boosting using external beam electrons, reduced field photon beams, intensity-modulated radiotherapy, interstitial brachytherapy, or intraoperative techniques are under evaluation (Graham and Fourquet 2006, Bondiau *et al* 2009). Unlike these techniques, the method of radiation delivery discussed in this work allows for an extremely large, ablative absorbed dose to be delivered to the lumpectomy cavity wall and surrounding stroma while minimizing absorbed dose to the rest of the healthy breast. This is important because, ultimately, dose escalation is limited by the volume of breast irradiated or the amount of absorbed dose received by adjacent critical normal tissues (ribs, lung, heart, etc.). Focal absorbed dose delivery is accomplished through direct intracavitary infusion of beta-emitting radionuclides (rhenium-186 [^{186}Re]/rhenium-188 [^{188}Re]) encapsulated by lipid nanoparticles (liposomes). Liposomes have been used as drug delivery vehicles for the treatment of human disease (Gabizon 2007) and are used in this method for improved retention within the injected region compared to non-liposomal compounds, thus increasing therapeutic ratio (Bao *et al* 2006, Harrington *et al* 2000, Oussoren and Storm 2001).

Important to the treatment of any disease is a simple relationship between treatment and effect. In external beam radiotherapy, mean absorbed dose has been used as such to predict tumor control and normal tissue toxicity. Improvements in treatment planning and radiation delivery techniques have allowed for the inclusion of radiobiological aspects, such as cell sensitivity, repair rates, potential doubling time, or dose heterogeneity, to supplement treatment optimization (Begg *et al* 1999, Rischin *et al* 2005, Tome and Fowler 2002). It is understood that the same mean absorbed dose delivered may not have the same biological dose response for all patients. In lieu of this, radiobiological indices can be implemented to allow for different treatment plans and modalities to be related to a known standard. The dosimetric characteristics of the method of radiation delivery in this work have previously been investigated for the simultaneous treatment of the lumpectomy cavity wall and draining lymph nodes (Hrycushko *et al* 2010). This study characterizes the treatment modality using radiobiological indices to assess effectiveness in sterilizing residual disease within the lumpectomy cavity wall and inhibiting the wound healing effect while also considering normal tissue toxicity. Effective uniform dose (EUD) and tumor control probability (TCP) were modeled to evaluate therapy effectiveness, while normal tissue complication probability (NTCP) and biological effective dose (BED) models were implemented to assess normal tissue toxicity of the ipsilateral breast and kidneys. Dosimetric and radiobiological index calculations were extrapolated from previous small animal imaging studies evaluating the treatment of a positive surgical margin of head and neck squamous cell carcinoma xenografts in rats using intraoperative infusion of ^{186}Re-liposomes (Wang *et al* 2008).

2. Methods

For modeling purposes, it was assumed that post-lumpectomy intracavitary infusion of the ^{186}Re/^{188}Re-liposomes would give a uniform intracavitary distribution of liposomes. The infused cavity was modeled to be 1.0 cm in diameter to represent the collapsed lumpectomy cavity following excision of T1–2 early stage breast cancer. The volume of the lumpectomy cavity is much smaller than the excised tumor and tumor-free margins due to a lack of tissue support within the cavity and has previously been discussed (Hrycushko *et al* 2010). Clearance rates were extrapolated from small animal imaging studies (Wang *et al* 2008). Dosimetric and radiobiological index calculation methods are described in the following subsections.

2.1. Absorbed dose calculations

The absorbed dose distribution within the breast (D; mGy) was calculated using the radionuclide dose point kernel (DPK) convolution method. The technique used has previously been described (Bao *et al* 2005) and only a brief explanation follows. Three-dimensional 500 × 500 × 500 matrices with voxel sizes of 0.2 × 0.2 × 0.2 mm^3 were formulated in Matlab (ver. 7.4.0.287 [R2007a]) to represent the lumpectomy breast. The EGSnrc (Kawrakow and Rogers 2000) Monte Carlo simulation user code EDKnrc (Rogers *et al* 2005) was used to calculate DPK matrices which included absorbed dose from photon and beta emissions (Burrows 1988, Stabin and da Luz 2002) of ^{186}Re and ^{188}Re radionuclides. DPKs of selected radionuclides, and monoenergetic photons and electrons were also calculated within a water medium for comparison with published DPKs (Mainegra-Hing *et al* 2005, Furhang *et al* 1996, Simpkin and Mackie 1990). The convolution of the DPK matrix (K; mGy/MBq-hr) with a cumulative activity matrix ($\tilde{A}$; MBq-hr) describing the lumpectomy cavity was calculated using Fourier transform (FT), multiplication (•), followed by inverse Fourier transform (iFT) (Bao *et al* 2005):

$$D(i,j,k) = \mathrm{iFT}\left\{\mathrm{FT}\left[K(i,j,k)\right] \cdot \mathrm{FT}\left[\tilde{A}(i,j,k)\right]\right\}. \quad (1)$$

2.2. Radiobiological index calculations

As a result of the intracavitary distribution of ^{186}Re/^{188}Re-liposomes, a non-uniform dose distribution is delivered within the lumpectomy cavity wall. The equivalent uniform dose (EUD) is the uniform absorbed dose that produces the same biological outcome as that which is delivered heterogeneously throughout the treatment volume (Niemierko 1997). In this work it is used to relate the large non-uniform dose distribution to an equivalent treatment using external beam radiotherapy (EBRT) delivering daily 2.0 Gy fractions within a few minutes for five fractions per week to mimic a conventional EBRT treatment regimen. Assuming the response of the tissue to be dependent on the clonogen-weighted mean of the voxels, the EUD was determined through the linear-quadratic model (Niemierko 1997, Butler *et al* 2009):

$$\mathrm{EUD} = \frac{-\ln\left[\frac{\sum_{i=1}^{N}\rho_i v_i \exp(-\alpha \cdot \mathrm{BED}_i)}{\sum_{i=1}^{N}\rho_i v_i}\right]}{\alpha + \beta d - \frac{1.4\gamma}{d}} \quad (2)$$

where d is the reference 2.0 Gy daily fraction, α and β characterize cell kill resulting from irreparable and repairable mechanisms, γ represents the reduction in cell killing due to repopulation, ρ_i and v_i are individual voxel clonogen density and volume and N is the total

number of voxels within the treatment volume. The biologically effective dose (BED) is typically used to quantitatively compare different patterns of radiation delivery. For this protracted irradiation, individual voxel BED_i were calculated (Butler *et al* 2009):

$$\begin{aligned}
&BED_i = D_{Teff,i} \times RE_{Teff,i} - \frac{\gamma \cdot T_{eff,i}}{\alpha} \\
&T_{eff,i} = \frac{1}{\lambda_{EC}} \ln\left(\frac{\alpha \cdot \dot{D}_{0,i}}{\gamma}\right) \\
&D_{Teff,i} = D_i\,[\,1 - \exp\,(-\lambda_{EC} \cdot T_{eff,i})] \\
&RE_{Teff,i} = 1 + \left(\frac{\beta}{\alpha}\right)\left[\left(\frac{2\,\dot{D}_{0,i} \cdot \lambda_{EC}}{(\mu - \lambda_{EC})\left[1 - \exp\left(-\lambda_{EC} \cdot T_{eff,i}\right)\right]}\right)\right] \times \left(\frac{1 - \exp\left(-2\lambda_{EC} \cdot T_{eff,i}\right)}{2\lambda_{EC}} - \frac{1 - \exp\left[-(\mu + \lambda_{EC})T_{eff,i}\right]}{\mu + \lambda_{EC}}\right)
\end{aligned} \tag{3}$$

where λ_{EC} is the effective clearance rate of the $^{186}Re/^{188}Re$-liposomes from the lumpectomy cavity and μ is the sublethal damage repair rate. Here, $D_{Teff,i}$ is the effective dose delivered within the effective treatment time, $T_{eff,i}$ (i.e., when cell repopulation rate equals cell kill rate), and $RE_{Teff,i}$ is the relative effectiveness per unit dose. The initial voxel dose rate, $\dot{D}_{0,i}$, was determined from the calculated dose matrix from (1)

$$\dot{D}_{0,i} = D_i \cdot \lambda_{EC}. \tag{4}$$

TCP, defined by a Poisson statistics model, is the probability of having no surviving clonogens. It is determined for the treatment volume by taking into account dose heterogeneity and the distribution of clonogens within the wall surrounding the lumpectomy cavity (Webb and Nahum 1993):

$$\begin{aligned}
TCP_i &= \exp\,[\,-\rho_i v_i \cdot \exp\,(-\alpha \cdot BED_i)] \\
TCP &= \prod_{i=1}^{N} TCP_i
\end{aligned} \tag{5}$$

where TCP_i is the voxel TCP.

In this work, the generalized EUD for the healthy breast (EUD_{hb}) was used in combination with NTCP to assess toxicity to the ipsilateral breast and was calculated as previously shown for normal tissue (Bovi *et al* 2007):

$$EUD_{hb} = \left[\sum_{i=1}^{N_{hb}} \frac{v_i}{V_0}\left(D_i^{1/n}\right)\right]^n \tag{6}$$

where V_0 is the total volume of healthy breast, n is a model parameter controlling the volume effect, and N_{hb} is the total number of voxels within the healthy breast. The NTCP Lyman model was then used with the EUD_{hb} index to quantify breast toxicity probability with the heterogeneous dose distribution (Lyman 1985):

$$\begin{aligned}
NTCP &= \frac{1}{\sqrt{2\pi}} \int_{-\infty}^{t_L} \exp\left(-x^2/2\right) dx \\
t_L &= \frac{EUD_{hb} - TD_{50}}{m - TD_{50}}
\end{aligned} \tag{7}$$

where TD_{50} is the tolerance dose for 50% complication probability and m is the inverse of the slope of the steepest part of the dose-response curve.

The results of a previous study suggested the kidney to be the dose-limiting organ of this modality (Wang *et al* 2008). The intra-organ activity distribution is unknown; thus, kidney toxicity in this work was determined by relating the predicted biologically effective dose of the kidney (BED_K) with the external beam dose which would give the same BED_K. An external beam dose of 28 Gy delivered in 1.0 Gy fractions was used as the kidney tolerance limit ($TD_{50/5}$) (Dawson *et al* 2010). The BED_K was calculated from the dose rate over time, which was determined by assuming linear, first-order kinetics for clearance from the lumpectomy cavity and uptake within the kidneys in similar fashion as in ICRP biokinetic models (ICRP 1979):

$$\frac{dA_K}{dt} = f\lambda_{BC}A_C - \lambda_{EK}A_K$$
$$A_K(t) = \frac{f\lambda_{BC}A_{C0}}{\lambda_{EK}-\lambda_{EC}}\left[\exp(-\lambda_{EC}\cdot t) - \exp(-\lambda_{EK}\cdot t)\right] \quad (8)$$

where A_K is the activity within the kidney over time and λ_{EK} is the effective clearance rate of activity from the kidney. Here, A_C is the activity within the lumpectomy cavity, f is the fraction of activity cleared from the cavity which gets transferred from the body fluids to the kidneys, and λ_{BC} is the biological clearance rate of the nanoparticles from the lumpectomy cavity. The biological clearance rate from the lumpectomy cavity was assumed similar as that for the intracavitary delivery of ^{186}Re-liposomes for head and neck squamous cell carcinoma xenografts in rats and determined to be approximately 50 h (Wang *et al* 2008). Effective clearance from the kidneys, λ_{EK}, was calculated by fitting (8) to the small animal kidney data of Wang *et al* (2008), which gave the percent injected activity at different times within rat kidneys, and minimizing the distance between (8) and the data points. The BED_K and kidney dose (D_K) were used with the clearance rates and determined in similar fashion as that of Howell *et al* (1994):

$$BED_K = D_K \times RE_K$$
$$RE_K = 1+\left(\frac{\beta}{\alpha}\right)_K\left[\frac{\Delta f T_{EK}T_{EC}A_{C0}}{m_K T_{BC}\ln(2)(T_{EC}-T_{EK})}\right]\left[\frac{2T_\mu^4(T_{EC}-T_{EK})}{(T_\mu^2-T_{EC}^2)(T_\mu^2-T_{EK}^2)}+\frac{2T_{EC}T_{EK}T_\mu}{(T_{EC}^2-T_{EK}^2)}\left(\frac{T_{EC}}{T_\mu-T_{EC}}+\frac{T_{EK}}{T_\mu-T_{EK}}\right)-\frac{T_\mu}{(T_{EC}-T_{EK})}\left(\frac{T_{EC}^2}{T_\mu-T_{EC}}+\frac{T_{EK}^2}{T_\mu-T_{EK}}\right)\right]$$
$$D_K = \frac{\Delta}{m_K}\left[\frac{T_{EC}^2T_{EK}^2}{\ln(2)T_{BC}(T_{EC}-T_{EK})(T_{EK}-T_{EC})}\right] \quad (9)$$

where Δ is the radionuclide specific equilibrium dose rate constant and m_K is the mass of reference man kidneys (ICRP 1979). Here, the half-time analogs of the clearance rates were used; T_μ is the repair halftime of kidney cells, T_{EC} is the effective halftime of the activity within the lumpectomy cavity, T_{BC} is the biological halftime within the lumpectomy cavity and T_{EK} is the effective halftime of the activity within the kidney. Then the external beam dose (D_K^{EBRT}) delivered in 1.0 Gy fractions of N fractions giving the same BED_K to the kidney was calculated using the kidney α/β_K (Dale 2004):

$$D_K^{EBRT} = Nd = \frac{BED_K}{1+d(\beta/\alpha)_K}. \quad (10)$$

2.3. Stroma

There is a large amount of cross-talk between the tumor and surrounding stroma which aids in the invasive nature of the tumor. As previously mentioned, the wound healing process has been shown to stimulate tumor growth. Treating the cavity wall to a large dose of radiation not only kills residual cancer cells within the vicinity, but also inhibits the wound healing stimulation and delays tumor growth (Belletti *et al* 2008). For this work, it was assumed that

suppression of the wound healing effect is proportional to the damage to the surrounding stromal tissue caused by the treatment. The stromal α/β_K ratio has been estimated to be 6.2 Gy (Begg and Terry 1984), a value generally between that considered for early and late responding tissues. If the ultimate goal is to cause stromal damage, it may be counterproductive to fractionate the treatment and allow for complete repair between fractions. This was evaluated for ^{188}Re-liposomes by comparing the external beam dose (D_s^{EBRT}) which would give the same BED as that at the therapeutic range (determined in dose calculations to be 5 mm; see below) versus the amount of injected activity within the cavity. The 5 mm distance was used for the BED reference because it is the lowest dose within the therapeutic range. This was calculated by setting the BED of the protracted treatment at 5 mm distance from the cavity wall equal to the BED of an external beam treatment given in 2.0 Gy fractions and solving for the total external beam absorbed dose:

$$D_s^{EBRT} = Nd = \frac{\frac{\dot{D}_{0,5.0mm}}{\lambda_{EC}}\left[1+\frac{\dot{D}_{0,5.0mm}}{(\mu+\lambda_{EC})(\alpha/\beta)_s}\right]}{1+d(\beta/\alpha)_s}. \quad (11)$$

Here, $\dot{D}_{0,5.0mm}$ is the initial dose rate seen at the therapeutic range (5.0 mm) for ^{188}Re-liposomes. The stromal repair halftime, T_μ, was unknown; thus, the equivalent external beam dose for increasing amounts of injected activity was plotted for different values of repair halftimes seen in mammalian tissues (0.5–3.0 h).

3. Results

3.1. Absorbed dose calculations

The absorbed dose distribution within the lumpectomy cavity wall was calculated assuming a 1.0 cm diameter to represent the post-lumpectomy cavity size of stage T1–T2 breast cancer. Figure 1 shows the absorbed dose distribution, as calculated with (1), when a uniform distribution of radionuclide encapsulated liposomes is injected within the lumpectomy cavity. The dose distributions are normalized to the dose at the cavity wall surface. At a distance of 2.0 mm and 5.0 mm, 1.12% and 0.61% the wall surface dose was received for ^{186}Re/^{188}Re-liposomes, respectively. These distances are taken to be the therapeutic range for these radionuclides, taking full advantage of the sharp decrease in absorbed dose with distance from the beta emissions. The dose at 1.0 cm distance from the cavity wall falls to 0.016% and 0.013% the cavity wall surface dose for ^{186}Re/^{188}Re-liposomes, respectively, and is primarily delivered as a result of photon emissions. Although a low percentage of the cavity wall surface dose is seen at 2 mm and 5 mm, a 50 Gy dose delivered at these distances implies that only a 0.7 Gy and a 1.0 Gy dose would be delivered at 1 cm distance from the cavity wall surface for ^{186}Re/^{188}Re-liposomes, respectively. These therapeutic ranges (2.0 mm for ^{186}Re; 5.0 mm for ^{188}Re) are appropriate for delivering sufficient absorbed dose for tumor cell kill while also displaying exceptional normal tissue sparing capability.

3.2. Radiobiological index calculations

Dosimetric and biological indices were calculated for ^{186}Re/^{188}Re-liposomes for an amount of injected activity required to deliver 50 Gy to the respective therapeutic ranges previously discussed. Table 1 provides symbol values used in calculations involving (2–7). These values were chosen among published values used for breast tumours; however, variation in individual parameters may impact resulting EUD and TCP calculations. For example, although α/β of 10 Gy was used in this report, it has been reported to be as low as 4.6 Gy (Bentzen *et al* 2008) for breast tumours. The percent difference between maximum and

minimum calculated EUD values was 27% for ^{186}Re and 9.2% for ^{188}Re when changing from an α/β of 3 Gy with α as low as 0.3 Gy^{-1} to an α/β of 10 Gy with α as high as 0.4 Gy^{-1}. The sensitivity of EUD to various model parameters has been investigated elsewhere (Ebert 2000). Table 2 shows that although a large average absorbed dose is given within the therapeutic range giving a high probability of tumour cell sterilization, the EUD values are much lower. This is due to the large heterogeneous dose distribution as well as the EUD calculation being heavily influenced by the lower doses received near the edge of the therapeutic range. One of the main benefits with this treatment technique is demonstrated with the minimal ipsilateral breast EUD_{hb}. In turn, the calculated NTCP is minimal at 0.046%, thus providing superior normal tissue sparing when compared to current methods of partial breast irradiation (Bovi *et al* 2007).

The above calculations assumed uniform residual clonogen densities throughout the therapeutic ranges, as is commonly done in EUD and TCP calculations. Considering a spherical lumpectomy cavity geometry, this assumption implies greater probability of residual tumor clonogens at larger distances from the cavity wall. Based on the nature of subclinical disease spread from primary tumor, it seems more likely residual tumor clonogen density would decrease with increasing distance from the lumpectomy cavity. This concept may be supported from the distribution of recurrences (90% being at or near the lumpectomy cavity wall (Tobias *et al* 2006)) and the distribution of tumor spread seen in mastectomy specimens (Gump 1992, Holland *et al* 1985). The non-uniform dose distributions from intracavitary radiation delivery may be preferential for a tumor cell density which decreases with distance from the cavity. With this in mind, it was important to model how treatment volume EUD may change with different clonogen distributions using (2). The tumor clonogen density distribution was modeled as a Lorentzian distribution function to give the capability of a steep drop-off in tumor clonogen density from the surface of the cavity wall. Figure 2 shows EUD indices calculated for the volume defined by the therapeutic range of ^{188}Re assuming different Lorentzian distributions of tumor clonogen density with distance from the cavity wall. The amount of tumor clonogens within the therapeutic range was kept constant at 10 000, a value representative of the number of residual tumor clonogens following lumpectomy surgery (Wyatt *et al* 2008). Figure 2 shows that a 15% increase in EUD was seen when over 90% of the residual clonogens were within 1.0 mm of the cavity wall surface compared with a uniform tumor clonogen density distribution. This increased EUD is support for an intracavitary radiation delivery technique for residual early stage breast cancer, being optimal for the distribution of recurrences seen in the clinical setting (Tobias *et al* 2006).

The absorbed dose and radiobiological index calculations of figure 1 and table 2 validated the therapeutic ranges of 2.0 mm and 5.0 mm for ^{186}Re/^{188}Re, respectively. However, it may be of interest to know how modeled EUD and TCP may change when considering different treatment volume sizes as well as for different quantities of infused activity. Figures 3(A) and (C) represent the change in EUD when the distance from the cavity center is considered the treatment volume for ^{186}Re/^{188}Re-liposomes, respectively. It is seen that a vertical asymptote is quickly approached for small treatment volumes surrounding the lumpectomy cavity. The absorbed dose is sufficient for essentially zero survival and (2) approaches infinite EUD. Figures 3(B) and (D) describe the change in calculated TCP for the same treatment volumes considered in figures 3(A) and (C). The TCP figures show the rapid drop in probability of tumor control with increased treatment volume size due to the quick drop-off in absorbed dose from the beta emissions of each radionuclide. As the amount of injected activity is increased, enough absorbed dose at larger distances is delivered by photon emissions to sterilize residual tumor clonogens. This is apparent from the gradual drop-off in EUD and TCP with increased treatment volume size for the largest quantities of infused activity.

3.3. Normal tissue toxicity

Of particular interest in therapy applications with liposomes, is toxicity to organs and tissue involved in the reticuloendothelial system (RES), such as the kidney, liver, and spleen. Activity within the kidney and liver following direct injection of ^{186}Re-liposomes to a positive surgical margin of head and neck squamous cell carcinoma xenografts models in rats has previously been observed (Wang *et al* 2008). Knowing the uptake and clearance patterns within these organs, absorbed dose may be estimated assuming similar kinetics following direct injection to the lumpectomy cavity of breast cancer patients. Due to the large size of the human liver and the significantly less amount of activity being retained in this organ (Wang *et al* 2008), only the kidney dose was considered here. Following (8–10), the external beam dose which gives the same kidney BED_K as that delivered from the radionuclides was calculated. The parameter values used for the calculations are shown in table 3. Once f and λ_{EK} were estimated from the data of Wang *et al* (2008) as described in the methods section, activity within the kidneys over time for ^{186}Re/^{188}Re-liposomes was predicted using (8). The data of Wang *et al* (2008) is plotted in figure 4, along with the derived fits from (8). Data for ^{188}Re-liposomes were extrapolated from the ^{186}Re-liposome data assuming the same biological uptake and clearance rates. The relationship between the amount of injected activity within the lumpectomy cavity and the equivalent external beam dose which would be delivered to the kidneys was determined from (10) and is shown in figure 5. Arrows are placed at the location of the $TD_{50,5}$ dose of 28 Gy as well as the location of the absorbed dose given to the kidney for the amount of injected activity for the treatment described in table 2. Figure 5 shows that a large amount of activity would need to be injected before kidney toxicity becomes an issue with this modality. This is due to the sustained retention of the liposomes within the lumpectomy cavity immediately following injection. The amount of injected activity for the treatment in table 2 was seen to deliver a small external beam equivalent kidney dose of 0.19 Gy and 0.12 Gy for^{186}Re/^{188}Re-liposomes, respectively.

Ipsilateral breast toxicity was evaluated from EUD_{hb} and NTCP calculations of (6–7). Figure 6 shows how EUD_{hb} and NTCP of the ipsilateral breast change with increasing concentration of injected activity of ^{186}Re/^{188}Re-liposomes. From figures 5 and 6, it is seen that kidney toxicity would occur before breast complications. An injected activity of 3.1 Ci and 6.1 Ci of ^{186}Re/^{188}Re-liposomes would reach the $TD_{50,5}$ of 28 Gy for the kidneys while only giving an NTCP of about 2.7% and 17% to the ipsilateral breast, well below the $TD_{50,5}$ endpoint of 70 Gy. At these extreme levels of infused activity other toxicity issues, such as with the low limiting dose to bone marrow, may also need to be considered.

3.4. Stroma

Stromal damage was considered to be proportional to the inhibition of the wound healing effect on tumor growth. The EBRT dose which would deliver the same BED_S at the therapeutic range edge of 5.0 mm from the lumpectomy cavity wall for ^{188}Re-liposomes for different amounts of injected activity is shown in figure 7. Although the BED_S at distances closer to the cavity would have higher values, this distance was considered because it is the minimum dose received within the therapeutic range. The repair rate for stromal cells during wound healing is unknown, thus figure 7 displays BED_S calculation results for the general range of repair times seen in mammalian cell lines. Figure 7 shows that an injected amount of activity over 100.0 mCi gives a biologically equivalent external beam dose of over 100.0 Gy delivered in daily 2.0 Gy fractions at 5.0 mm distance. This level of EBRT dose may not be feasible in a daily fraction regimen due to time constraints and cell repopulation and an accelerated regimen such as that reported in this work may be more appropriate. It is important to consider the biological consequences of the large dose levels achieved in close proximity to the cavity wall surface. Similar to all seed, interstitial catheter, or balloon

brachytherapy, where dose is prescribed to the PTV edge, absorbed dose is much higher towards the source. By delivering 50 Gy at the edge of the therapeutic range with this technique, over 4600 Gy and 8100 Gy are delivered to the cavity wall surface for ^{186}Re- and ^{188}Re-liposomes, respectively. Not only are residual tumor cells ablated, but supporting stromal cells of which secrete growth factors and cytokines as part of the wound healing response. Intraoperative irradiation of the lumpectomy cavity wall using the TARGIT technique has been shown to suppress the stimulatory effect of the wound fluid on tumor growth (Belletti *et al* 2008).

4. Discussion

The aim of this work was to characterize the treatment of residual early stage breast cancer with direct intracavitary infusion of ^{186}Re/^{188}Re-liposomes by using dosimetric and radiobiological indices. Further evaluation is warranted with the use of small animal studies before extended for clinical use. This work provided consideration to treatment volume size for each radionuclide and how increased infused activity concentrations may affect treatment volume decisions. Radiobiological indices were used to assess therapy effectiveness and normal tissue complication by comparison with typical EBRT treatment protocol. It was seen, through modeling of a spherical lumpectomy cavity, that a therapeutic range of 2.0 mm and 5.0 mm for ^{186}Re- and ^{188}Re-liposomes is adequate in achieving therapeutic absorbed dose levels. These therapeutic ranges take advantage of delivering a focally large dose within these distances through beta emissions while allowing for a steep drop-off in absorbed dose within a few millimeters further, thus minimizing dose to the rest of the healthy breast. The dosimetric and radiobiological index characterization of this work was for a 1 cm diameter lumpectomy cavity. Previous work has shown that for the same amount of injected activity larger lumpectomy cavities receive lower absorbed dose distributions within the wall and surrounding tissue due to less crossfire dose (Hrycushko *et al* 2010). This would not only reduce the therapeutic effect in the cavity wall and stroma due to the dose dependence of (2–5, 11), but also reduce the breast toxicity from (6–7). An increase in injected activity would likely be required for larger lumpectomy cavities. This would increase the dose received by the kidneys; however, figure 5 shows kidney toxicity to be minimal.

Therapy modalities today are treating more and more early stage breast cancer, allowing for women to live much longer disease-free lives. The amount of radiation delivered to the ipsilateral breast along with extended post-treatment life spans increases the risk of cancer induction from the treatment process itself. The tissue sparing capacity of this method delivers minimal dose to the ipsilateral breast, thus reducing the cancer induction capacity of the radiation when following a stochastic effects approach to radiation exposure. Furthermore, the breast tissue sparing allows for the possibility of treating recurrences with the same method. Recurrences following most breast conserving treatment regimens are treated with mastectomy because the breast tissue cannot handle additional radiation damage. With this method of radiation delivery, the breast tissue receives such minimal absorbed dose levels that detected recurrences may possibly be treated with spot injections without causing further breast tissue complications.

Liposomes are used similar to brachytherapy seeds to encapsulate the therapeutic radionuclides. They also provide the benefit of allowing surface alterations to tailor treatments to specific needs, such as increasing retention or improving upon in vivo uptake distributions. Or the surface of the liposomes may be labeled with antibodies to target over expressed receptors of specific cancer cells. This may be used to improve the biological clearance time or to treat systemically for tumor spread. Liposomes have already been investigated for use in lymph node mapping and sentinel lymph node detection (Chu *et al*

2010). They are taken up by the lymph vessels, are filtered and accumulate within the lymph nodes, as do cancer cells. The same radionuclide encapsulated liposomes infused to the lumpectomy cavity may possibly be used to treat draining lymph nodes sentinel lymph nodes for isolated tumor cells or micrometastases (Hrycushko *et al* 2010). It seems logical that the recurrence rates for early stage breast cancer may approach 0% by treating the locations of highest probability of residual tumor cells and growth stimulating factors; however, much more research is needed to fully understand the relationship between the surgical wound and location of breast cancer recurrences.

5. Conclusions

Absorbed dose and biological index calculations demonstrate the effectiveness of direct intracavitary injections of ^{186}Re/^{188}Re-liposomes for treating post-lumpectomy residual early stage breast cancer. Focally ablative absorbed dose levels are achievable within the cavity wall which are unattainable with external beam delivery in 2.0 Gy daily fractions due to time constraints and normal tissue toxicity issues. Possible normal tissue complication pathways with this method of radiation delivery were evaluated and shown to be minimal. The immediate irradiation of the stroma through this protracted modality is expected to target microscopic spread and inhibit signaling from the wound healing response, thus reducing probability of local recurrence and cancer cell migration.

Acknowledgments

This work was financially supported by the Susan G Komen for the Cure®, BCTR0707169 and the National Cancer Institute (NCI) of NIH, R01 CA131039. BA Hrycushko was supported by the National Institute of Biomedical Imaging and Bioengineering (NIBIB) of NIH training grant, T-32 EB000817.

References

Alexander M A R, Brooks WA, Blake SW. Normal tissue complication probability modeling of tissue fibrosis following breast radiotherapy. Phys. Med. Biol. 2007; 52:1831–43. [PubMed: 17374914]

Bao A, Phillips W T, Goins B, Zheng X, Sabour S, Natarajan M, Woolley F R, Zavaleta C, Otto RA. Potential use of drug carried-liposomes for cancer therapy via direct intratumoral injection. Int. J. Pharm. 2006; 316:162–9. [PubMed: 16580161]

Bao A, Zhao X, Phillips W T, Woolley F R, Otto R A, Goins B, Hevezi JM. Theoretical study of the influence of a heterogeneous activity distribution on intratumoral absorbed dose distribution. Med. Phys. 2005; 32:200–8. [PubMed: 15719971]

Begg AC, Terry NH. The sensitivity of normal stroma to fractionated radiotherapy measured by a tumour growth rate assay. Radiother. Oncol. 1984; 2:333–41. [PubMed: 6084258]

Begg AC, et al. The value of pretreatment cell kinetic parameters as predictors for radiotherapy outcome in head and neck cancer: a multicenter analysis. Radiother. Oncol. 1999; 50:13–23. [PubMed: 10225552]

Belletti B, et al. Targeted intraoperative radiotherapy impairs the stimulation of breast cancer cell proliferation and invasion caused by surgical wounding. Clin. Cancer Res. 2008; 14:1325–32. [PubMed: 18316551]

Bentzen SM, et al. The UK Standardization of Breast Radiotherapy (START) Trial A of radiotherapy hypofractionation for treatment of early breast cancer: a randomized trial. Lancet Oncol. 2008; 9:331–41. [PubMed: 18356109]

Blichert-Toft M, Nielson M, During M, Moller S, Rank F, Overgaard M, Mouridsen HT. Long-term results of breast conserving surgery versus mastectomy for early stage invasive breast cancer: 20-year follow-up of the Danish randomized DBCG-82TM. protocol Acta Oncol. 2008; 47:672–81.

Bondiau P Y, Bahadoran P, Lallement M, Birtwisle-Peyrottes I, Chapellier C, Chamorey E, Courdi A, Quielle-Roussel C, Thariat J, Ferrero J. Robotic stereotactic radioablation concomitant with

neoadjuvant chemotherapy for breast tumors. Int. J. Radiat. Oncol. Biol. Phys. 2009; 75:1041–7. [PubMed: 19386428]

Bovi J, Qi S X, White J, Li XA. Comparison of three accelerated partial breast irradiation techniques: treatment effectiveness based upon biological models. Radiother. Oncol. 2007; 84:226–32. [PubMed: 17692980]

Burrows T, W. The program RADLST *Report BNL-NCS-52142*. Brookhaven National Laboratory; Upton, NY: 1988.

Butler W M, Stewart RR, Merrick GS. A detailed radiobiologic and dosimetric analysis of biochemical outcomes in a case-control study of permanent prostate brachytherapy patients. Med. Phys. 2009; 36:776–87. [PubMed: 19378738]

Chu M, Zhuo S, Xu J, Sheng Q, Hou S, Wang R. Liposome-coated quantum dots targeting the sentinel lymph node. J. Nanopart. Res. 2010; 12:187–97.

Dale R. The use of the linear-quadratic radiobiological model for quantifying kidney response in targeted radiotherapy Cancer. Biother. Radiopharm. 2004; 19:363–70.

Dawson L A, Kavanagh B D, Paulino A C, Das S K, Miften M, Li X A, Pan C, Ten Haken RK, Schultheiss TE. Radiation-associated kidney injury. Int. J. Radiat. Oncol. Biol. Phys. 2010; 76:S108–15. [PubMed: 20171504]

Ebert M A. Viability of the EUD and TCP concepts as reliable dose indicators. Phys. Med. Biol. 2000; 45:441–57. [PubMed: 10701514]

Fisher B, Anderson S, Bryant J, Margolese R G, Deutsch M, Fisher E R, Jeong J, Wolmark N. Twenty-year follow-up of a randomized trial comparing total mastectomy, lumpectomy, and lumpectomy plus irradiation for the treatment of invasive breast cancer. N. Engl. J. Med. 2002; 347:1233–41. [PubMed: 12393820]

Furhang E E, Sgouros G, Chui CS. Radionuclide photon dose kernels for internal emitter dosimetry. Med. Phys. 1996; 23:759–64. [PubMed: 8724750]

Gabizon A, A. Applications of liposomal drug delivery systems to cancer therapy *Nanotechnology for Cancer Therapy*. MAmiji, M., editor. CRC Press; Boca Raton, FL: 2007. p. 595-611.

Graham P, Fourquet A. Placing the boost in breast-conservation radiotherapy: a review of the role, indications and techniques for breast-boost radiotherapy. Clin. Oncol. (R. Coll. Radiol.). 2006; 18:210–9. [PubMed: 16605052]

Guerrero M, Li XA. Analysis of a large number of clinical studies for breast cancer radiotherapy: estimation of radiobiological parameters for treatment planning. Phys. Med. Biol. 2003; 48:3307–26. [PubMed: 14620060]

Gump F E. Multicentricity in early breast cancer. Semin. Surg. Oncol. 1992; 8:117–21. [PubMed: 1496220]

Harrington K J, Rowlinson-Busza G, Syrigos K N, Uster P S, Vile RG, Stewart JS. Pegylated liposomes have potential as vehicles for intratumoral and subcutaneous drug delivery. Clin. Cancer Res. 2000; 6:2528–37. [PubMed: 10873109]

Hockel M, Dornhofer N. The hydra phenomenon of cancer: why tumors recur locally after microscopically complete resection. Cancer Res. 2005; 65:2997–3002. [PubMed: 15833823]

Holland R, Connolly J L, Gelman R, Mravunac M, Hendriks J, Verbeek A, Schnitt S J, Silver B, Boyages J, Harris JR. The presence of an extensive intraductal component following a limited excision correlates with prominent residual disease in the remainder of the breast. J. Clin. Oncol. 1990; 8:113–8. [PubMed: 2153190]

Holland R, Veling S H, Mravunac M, Hendriks J. Histologic multifocality of Tis, T1–2 breast carcinomas. Implications for clinical trials of breast-conserving surgery. Cancer. 1985; 56:979–90. [PubMed: 2990668]

Howell R W, Goddu SM, Rao DV. Application of the linear-quadratic model to radioimmunotherapy: further support for the advantage of longer-lived radionuclides. J. Nucl. Med. 1994; 35:1861–9. [PubMed: 7965170]

Hrycushko B A, Li S, Shi C, Goins B, Liu Y, Phillips W T, Otto PM, Bao A. Postlumpectomy focal brachytherapy for simultaneous treatment of surgical cavity and draining lymph nodes. Int. J. Radiat. Oncol. Biol. Phys. 2010 2010 Sep. 23.

International Commission on Radiological Protection (ICRP). Limits for intakes of radionuclides by workers. ICRP Publication 30 Part 1. Ann. ICRP. 1979; 2(3/4)

Kawrakow, I.; Rogers, DW. The EGSnrc code system: Monte Carlo simulation of electron and photon transport *Technical Report PIRS-701*. National Research Council of Canada; Ottawa: 2000.

Liljegren G, Holmberg L, Bergh J, Lindgren A, Tabar L, Nordgren H, Adami HO. 10-year results after sector resection with or without postoperative radiotherapy for stage I breast cancer: a randomized trial. J. Clin. Oncol. 1999; 17:2326–33. [PubMed: 10561294]

Lyman J T. Complication probability as assessed from dose volume histograms. Radiat. Res. 1985; 104:S13–9.

Mainegra-Hing E, Rogers DW, Kawrakow I. Calculation of photon energy deposition kernels and electron dose point kernels in water. Med. Phys. 2005; 32:685–99. [PubMed: 15839340]

Mannino M, Yarnold J. Effect of breast-duct anatomy and wound healing responses on local tumour recurrence after primary surgery for early breast cancer. Lancet Oncol. 2009; 10:425–9. [PubMed: 19341974]

Motomura K, Koyama H, Noguchi S, Inaji H, Kasugai T, Nagumo S. Malignant seeding of the lumpectomy cavity upon breast-conserving surgery. Oncology. 1999; 57:121–6. [PubMed: 10461058]

Niemierko A. Reporting and analyzing dose distributions: a concept of equivalent uniform dose. Med. Phys. 1997; 24:103–10. [PubMed: 9029544]

Oussoren C, Storm G. Liposomes to target the lymphatics by subcutaneous administration. Adv. Drug Deliv. Rev. 2001; 50:143–56. [PubMed: 11489337]

Rischin D, Peters L, Fisher R, Macann A, Denham J, Poulsen M, Jackson M, Kenny L, Penniment M, Corry J, Lamb D, McClure B. Tirapazamine, Cisplatin, and radiation versus Fluorouracil, Cisplatin, and radiation in patients with locally advanced head and neck cancer: a randomized phase II trial of the Trans-Tasman Radiation Oncology Group (TROG 98.02). J. Clin. Oncol. 2005; 23:79–87. [PubMed: 15625362]

Rogers D, W.; Kawrakow, I.; Seuntjens J, P.; Walters, BRB.; Mainegra-Hing, E. NRC user codes for EGSnrc *Technical Report PIRS-702*. National Research Council of Canada; Ottawa: 2005.

Sabel M S, Rogers K, Griffith K, Jagsi R, Kleer C G, Diehl K A, Breslin T M, Cimmino V M, Chang AE, Newman LA. Residual disease after re-excision lumpectomy for close margins. J. Surg. Oncol. 2009; 99:99–103. [PubMed: 19065638]

Simpkin DJ, Mackie TR. EGS4 Monte Carlo determination of the beta dose kernel in water. Med. Phys. 1990; 17:179–86. [PubMed: 2333044]

Stabin MG, da Luz L. Decay data for internal and external dose assessment. Health Phys. 2002; 83:471–5. [PubMed: 12240721]

Tagliabue E, et al. Role of HER2 in wound-induced breast carcinoma proliferation. Lancet. 2003; 362:527–33. [PubMed: 12932384]

Tobias J S, Vaidya J S, Keshtgar M, Douek M, Metaxas M, Stacey C, Sainsbury R, D'Souza D, Baum M. Breast-conserving surgery with intra-operative radiotherapy: the right approach for the 21st century? Clin. Oncol. (R. Coll. Radiol.). 2006; 18:220–8. [PubMed: 16605053]

Tome WA, Fowler JF. On cold spots in tumor subvolumes. Med. Phys. 2002; 29:1590–8. [PubMed: 12148742]

Veronesi U, Cascinelli N, Mariani L, Greco M, Saccozzi R, Luini A, Aguilar M, Marubini E. Twenty-year follow-up of a randomized study comparing breast-conserving surgery with radical mastectomy for early breast cancer. N. Engl. J. Med. 2002; 347:1227–32. [PubMed: 12393819]

Wang S X, Bao A, Herrera S J, Phillips W T, Goins B, Santoyo C, Miller FR, Otto RA. Intraoperative ^{186}Re-liposome radionuclide therapy in a head and neck squamous cell carcinoma xenograft positive surgical margin model. Clin. Cancer Res. 2008; 14:3975–83. [PubMed: 18559620]

Webb S, Nahum AE. A model for calculating tumour control probability in radiotherapy including the effects of inhomogeneous distributions of dose and clonogenic cell density. Phys. Med. Biol. 1993; 38:653–66. [PubMed: 8346278]

Wyatt R M, Jones BJ, Dale RG. Radiotherapy treatment delays and their influence on tumour control achieved by various fractionation schedules. Br. J. Radiol. 2008; 81:549–63. [PubMed: 18378526]

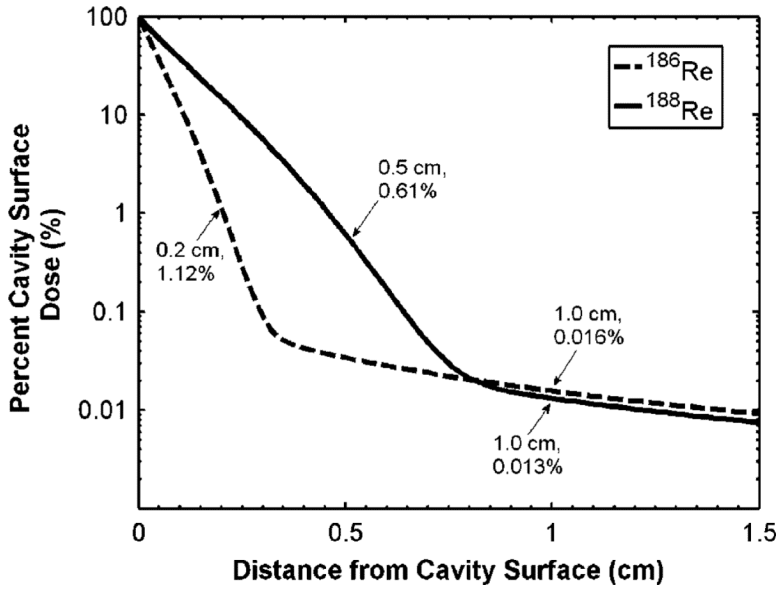

Figure 1.
Absorbed dose versus distance from wall surface of a 1.0 cm diameter lumpectomy cavity displayed as a percentage of the cavity wall surface dose.

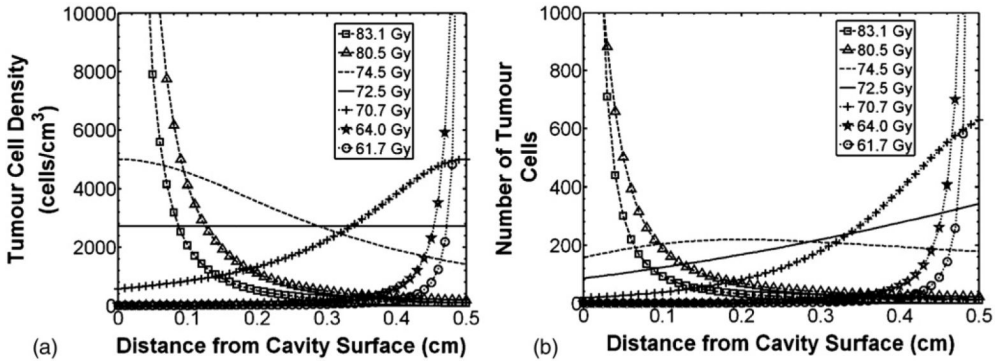

Figure 2.

^{188}Re EUD for different tumor clonogen distributions following a Lorentzian probability function outside the lumpectomy cavity wall surface (totaling 10 000 clonogens). The solid line represents uniform tumor clonogen density within the therapeutic range. (a) Tumor clonogen density distribution, and (b) Number of tumor clonogens with distance from cavity surface using densities from (2a).

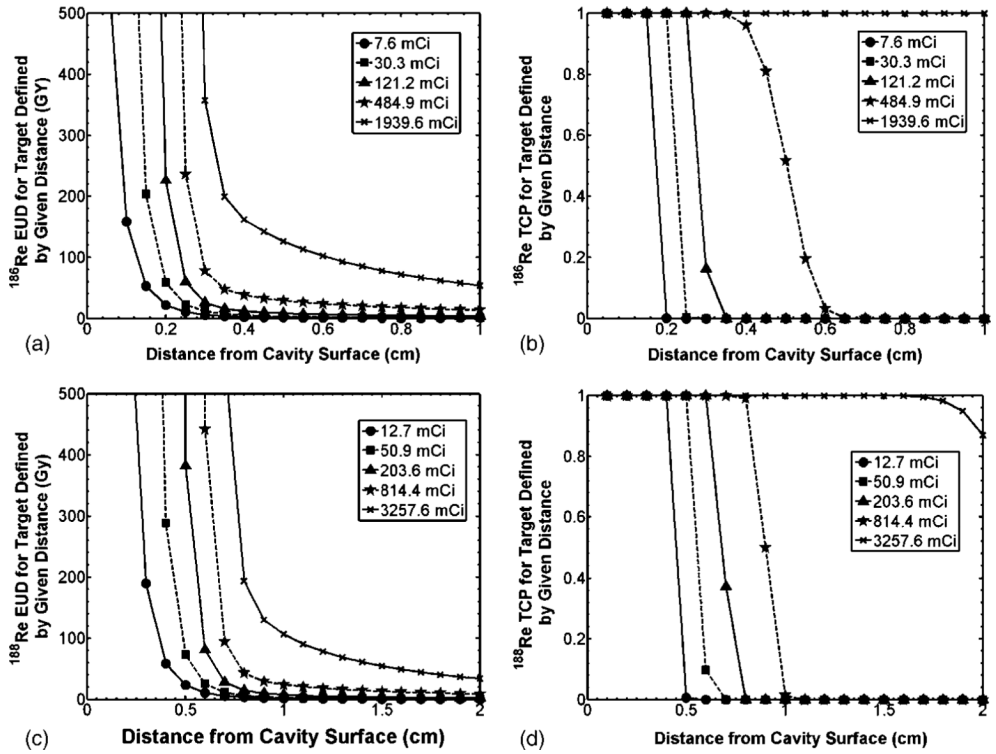

Figure 3.

EUD and TCP for different treatment volumes, as defined by the distance from the lumpectomy cavity surface, as well as varied injected activity. (a) and (c) represent calculated EUD values and (b) and (d) represent calculated fractional TCP values for ^{186}Re/^{188}Re-liposomes, respectively. Dashed lines with square markers refer to the infused activities for the modeled treatment of table 2.

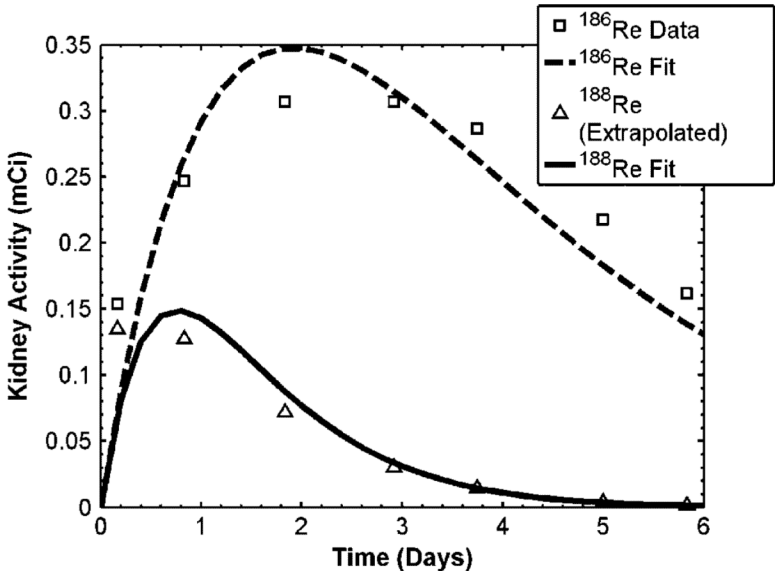

Figure 4.

Activity versus time within the kidney following intracavitary liposome infusion. Square data points are from Wang *et al* (2008) for ^{186}Re-liposomes. Triangle points represent the ^{186}Re-liposome data extrapolated to ^{188}Re-liposomes using the ^{188}Re physical decay halftime. Fitted lines were used to determine f and λ_{EK} by solving (8).

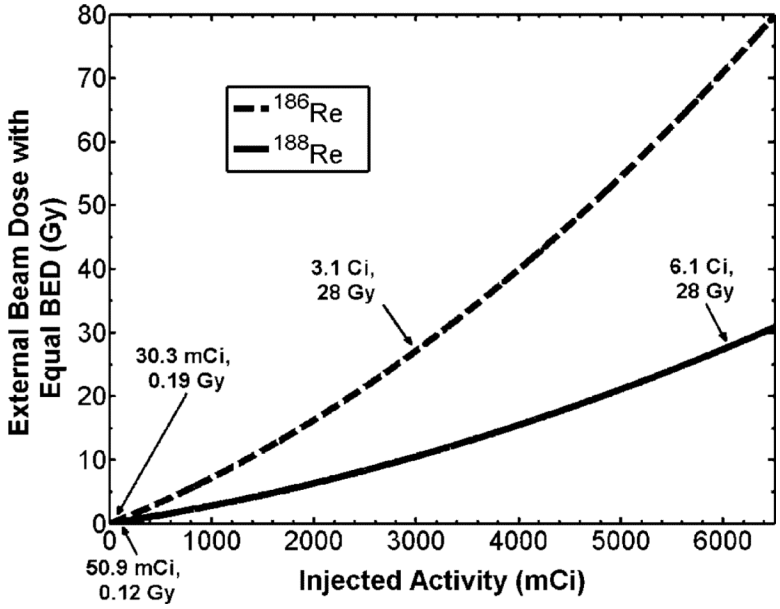

Figure 5.

External beam dose given to kidney giving same BED_K as $^{186}Re/^{188}Re$-liposomes. Arrows point to infused activity levels for the treatment shown in table 2 as well as the required infused activity levels to reach the $TD_{50,5}$ of 28 Gy.

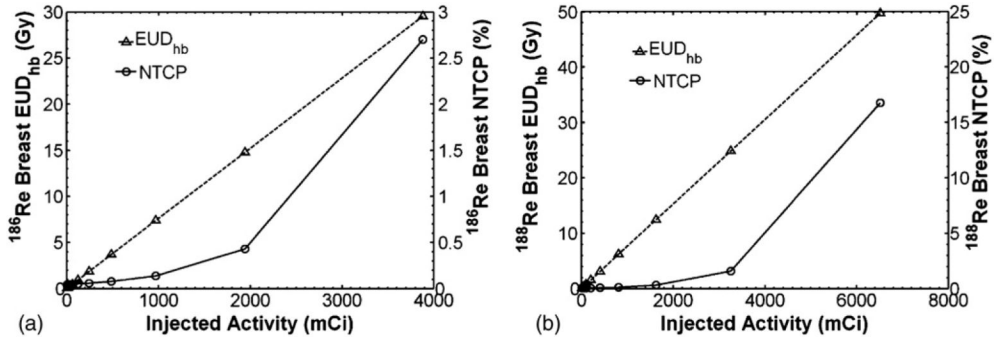

Figure 6.

EUD_{hb} and NTCP for ipsilateral breast versus injected activity for (a) ^{186}Re-liposomes and (b) ^{188}Re-liposomes.

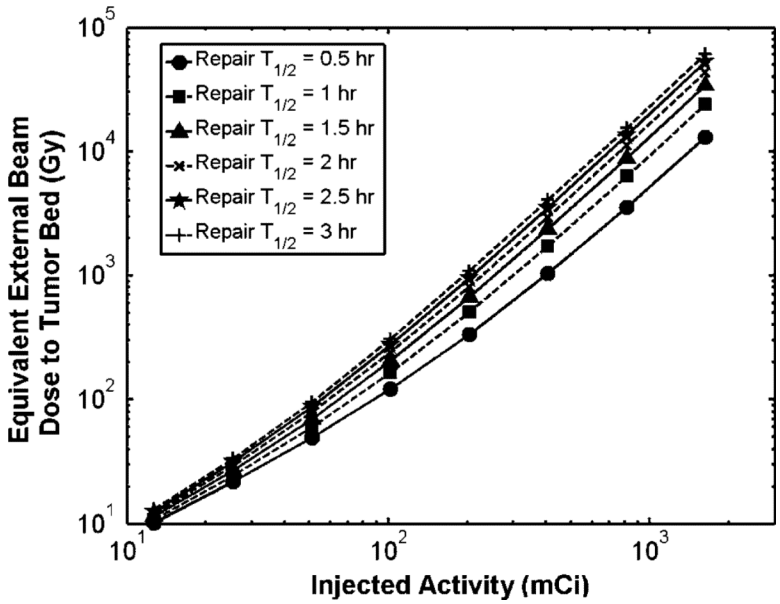

Figure 7.

External beam dose delivered in daily 2.0 Gy fractions required to deliver same BED_S at the 5 mm therapeutic range edge for ^{188}Re-liposomes versus injected activity.

Table 1

Symbol values used in calculations of (2–7).

Symbol	Simulation values
α_{tumour} [a]	0.3 Gy^{-1}
β_{tumour} [a]	0.03 Gy^{-2}
γ [a]	0.0462 $days^{-1}$
d	2Gy
$\lambda_{\text{EC Re-186}}$ [b]	0.5263 $days^{-1}$
$\lambda_{\text{EC Re-188}}$ [b]	1.3178 $days^{-1}$
μ [c]	0.0288 $days^{-1}$
n [d]	0.78
m [a]	0.3
$TD_{50,5\ \text{breast}}$ [a]	70 Gy

[a] Bovi *et al* 2007.

[b] Wang *et al* 2008.

[c] Guerrero and Li 2003.

[d] Alexander *et al* 2007.

Table 2

Dosimetric and radiobiological indices for ^{186}Re/^{188}Re-liposomes delivering 50 Gy at respective treatment distances.

Index	^{186}Re	^{188}Re
Injected activity	30.3 mCi	50.9 mCi
HBV[a]	998.56 cc	995.81 cc
TV[b]	0.91 cc	3.66 cc
EUD	58.2 Gy	72.5 Gy
EUD_{hb}	0.23 Gy	0.39 Gy
TCP	0.9999	1
NTCP	0.046%	0.046%
Avg. $dose_{tv}$	1596.1 Gy	1338.7 Gy
Avg. $dose_{breast}$	0.12 Gy	0.23 Gy
Therapeutic range	2 mm	5 mm
Therapeutic range dose	50 Gy	50 Gy
Dose 1 cm from therapeutic range	0.56 Gy	0.61 Gy

[a]HBV = healthy breast volume.

[b]TV = treatment volume.

Table 3

Symbol values used in calculations of (8–11).

Symbol	Simulation values
α/β_{K} [a]	2.6 Gy
α/β_{S} [b]	6.2 Gy
f [c]	0.3
$\lambda_{\text{EK Re-186}}$ [c]	0.52 days^{-1}
$\lambda_{\text{EK Re-188}}$ [c]	1.31 days^{-1}
m_{K} [d]	310g
T_{BC} [e]	2.08 days
$T_{\text{EC Re-186}}$ [e]	1.34 days
$T_{\text{EC Re-188}}$ [e]	0.53 days
T_{μ} [a]	0.12 days
$TD_{50,5\ \text{kidney}}$ [f]	28 Gy
$\Delta_{\text{Re-186}}$	7.12Gy-g/(mCi-hr)
$\Delta_{\text{Re-188}}$	16.54 Gy-g/(mCi-hr)

[a] Dale 2004.

[b] Begg and Terry 1984.

[c] Solved for using (8) and data from Wang *et al* 2008.

[d] ICRP 1979.

[e] Wang *et al* 2008.

[f] Dawson *et al* 2010.